

# **Influences of surface adsorption on field emission performances for W, Pt/Ir and multi-wall carbon nanotube emitters**

**Changkun Dong<sup>1,2</sup>, Mool C. Gupta<sup>1</sup>, G. Rao Myneni<sup>3</sup>**

<sup>1</sup> Applied Research Center, Old Dominion University, Newport News, VA 23606

<sup>2</sup> Physics Department, Old Dominion University, Norfolk, VA 23529

<sup>3</sup> Accelerator Division, Jefferson Lab, Newport News, VA 23606

Several surface adsorptions related field emission behaviors were investigated for W, Pt/Ir metal tips and multi-wall carbon nanotubes (MWNT). With the help of Fowler-Nordheim theory, we show clearly that there exists a stabilization process of the surface effective work function for W, Pt/Ir and MWNT emitters during emitting. Joule heating from electron emission may desorb the adsorbates on the emission sites of the metal emitter. We observed large emission current variation for MWNT emitters when they were tested after exposure to atmosphere. We suggest that there exist two different surface reaction modes in initial emission period, which are H<sub>2</sub>O and H<sub>2</sub> dominated processes respectively. An emission-adsorption equilibrium state may form stronger surface-adsorbate bonds. Nitrogen gas is a good protecting environment to maintain emission stability during the vacuum-atmosphere cycle. Operation of MWNT emitters under hydrogen atmosphere may improve the emission, which could be related to the modification of the surface work function. We suggest that surface adsorbate participated reaction is the dominated factor for the emission loss.

## I. INTRODUCTION

Field emission materials research is becoming an important area in vacuum microelectronics. The revolution from early electrochemical etched single metal tips to micro techniques integrated Spindt type emitter arrays, brings field emission cathode into the center stage of vacuum microelectronics. The requirements for low emission field and high emission stability limit the further uses of metal and Spindt type emitters due to the un-recovery of the emission site damage by ion sputtering. The emission stabilities of metal emitters have been thoroughly studied<sup>1, 2, 3, 4</sup>. Surface adsorption states that are subject to change under different emitter operation modes play a crucial role in the emission stability, reproducibility and lifetime for metal emitters. There are fewer reports about the adsorption changes affecting emission characteristics based on Fowler-Nordheim theory. In recent years, carbon nanotube (CNT) based field emitters have shown promising emission results under rigorous vacuum conditions<sup>5, 6, 7, 8</sup>. It is necessary to investigate the influences of surface adsorption on emission performance for CNT emitters comprehensively.

In this paper, we focus on the surface adsorption related emission behaviors. With the help of Fowler-Nordheim theory, changes of the emitter surface adsorption states were analyzed for W, Pt/Ir and MWNT emitters. Emission stabilities of MWNT emitters under various vacuum and/or operations conditions were also investigated.

## II. EXPERIMENTAL DETAILS

The tungsten tips were fabricated by two-step electrochemical etching. In first step, a 0.25 mm diameter tungsten wire was etched to 0.075 mm by 10% KOH solution, then

ultra-sharp W tip was etched out from 0.075mm wire in 1.5% KOH solution. The tip radius was calculated to be 7nm<sup>9</sup>. Pt/Ir emitter was commercial STM tip from Digital Instruments Company with tip radius around 50 nm by same calculation. Two groups of MWNT emitters were investigated. First group samples were fabricated by our thermal CVD at 700 °C using C<sub>2</sub>H<sub>2</sub>/Ar gas flow, and second group was commercial MWNT samples from NanoLab Co., as shown in Fig. 1. Emission performance was tested in a Varian Turbo V250 high vacuum system and a vacuum calibration system with base pressure of 1.6 x 10<sup>-11</sup> Torr. A SRS residual gas analyzer and Leybold Inficon 520 extractor gauges were used for vacuum measurements.

### III. RESULTS AND DISCUSSIONS

#### A. Effects of surface adsorption states

From Fowler-Nordheim theory<sup>10</sup>, the current density J is given by:

$$J = (1.54 \times 10^{-6} F^2 / \varphi) \exp(-6.83 \times 10^7 \varphi^{3/2} / F), \quad (1)$$

where J is the current density, F is the field on the emitter and  $\varphi$  is the surface effective work function which may be different from the intrinsic work function and is subject to change because of surface chemical state variations<sup>9</sup>. F is affected by multi-factors and can be formulated as  $F = \beta F_0$ , where  $\beta$  represents the field enhancement factor.  $F_0$  is the global electric field given by  $F_0 = V/d$ , where V is the applied voltage and d is the gap in the field emission diode configuration. Fowler-Nordheim equation can be expressed in terms of emission current I and applied voltage V<sup>11</sup>

$$I = a V^2 \exp(-b/V), \quad (2)$$

where  $a = 1.56 \times 10^{-6} \alpha \beta / (1.1 \phi) \exp(10.4 / \phi^{1/2})$ ,  $b = 6.44 \times 10^7 \phi^{3/2} / \beta$  and  $I = J \alpha$  with  $\alpha$  representing the emitting area.  $\beta$  is determined by factors of emitter surface morphology, potential applied and the distance between the emitter and the anode. A plot of  $\ln(I/V^2)$  versus  $1/V$  results in a straight line with slope  $-b$ , then analysis of the slope reveals the information about the surface work function. Electrons generally emit from some certain sites on the emitter surface, and this is confirmed by the switching of the emission sites at low currents level, even for the CNT emitter<sup>12</sup>. In the analysis of the surface state change by F-N theory, the relative emission inhomogeneity of the tip before and after adsorption must be considered. Generally the contact potential anisotropies are insufficient to alter the relative position of the various regions, that is, the regions contributing most to emission still are the ones after adsorption<sup>1</sup>. Another factor that influence the  $\beta$  is the emitter shape change because of the migration of surface atoms during emission<sup>13</sup>, it is reasonable to neglect this growth for short-term emission. After evaluating the effects of emission sites and the variations of the surface morphology,  $\beta$  is considered as constant with fixed tip-anode distance. Then  $b$  will reflect the change of the effective work function.

Figure 2 shows the F-N plots for W, Pt/Ir and MWNT emitters. In the current-voltage (I-V) measurements, typical the current data were recorded two minutes after raising the voltage. Before the I-V tests for W and Pt/Ir emitters, the system was pumped and baked at  $\sim 220$  °C for 8 hours and 18 hours respectively, and the system pressure is below  $5 \times 10^{-9}$  Torr. Figure 2(a) shows the F-N plots from three consecutive I-V tests for a tungsten tip. There are significant differences of the slopes between first curve and other two consecutive curves. This means the declining of the surface effective work function

during emission. It is known that the contamination by air often leaves a strong bonded adsorbed oxygen layer, which always acts to increase the work function, as oxygen being electronegative<sup>14</sup>. Surface oxygen is desorbed in two successive stages or "layers" at about 700°C and 1400°C respectively<sup>15</sup>. High temperature annealing<sup>16</sup> or providing a pulse of current<sup>3</sup> may desorb some of the contaminations and stabilize the emission. Obviously baking of the samples at 200 °C is not enough. The F-N slopes comparison of our results shows that the emitter surface adsorption state may reach a stable level after the initial emission period, which is believed being the result of the desorptions of contaminations caused by the emitter temperature rise from Joule heating during emitting. Obviously it is necessary that there should be a pre-running period in order to acquire stable surface conditions after baking the samples at low temperatures. Similar behavior may be observed for the Pt/Ir tip as shown in Fig.2 (b). The stabilization process of the surface adsorption was clearly shown from test 1 to test 3. At the same time, the system pressure variations were analyzed for Pt/Ir tip under the same emission current of 2μA during five I-V test cycles. Figure 3 shows that there was a much larger pressure increase in test 1 as compared to test 2-5. During first test, the pressure increase caused by degassing reached to  $2 \times 10^{-8}$  Torr. The degassing tended to be stable from test 3 and the pressure rises are only one-fifth the value of the first test. Even such pressure increase was partly caused by the gas desorption from the electron collector by the electron bombardment, Figure 3 still shows the basic desorption process which is consistent with change in the process of the surface effective work function. Some tests also showed that surface effective work function increased after desorption of the contaminations, especially for Pt/Ir tips. This may contribute to the inertness of Pt/Ir to oxidation and the

surface contaminations could be hydrogen dominant. Surface hydrogen may decrease effective work functions<sup>17</sup>, therefore it is probably that the Pt/Ir emitter surface adsorption state is highly governed by its history where either O or H plays key role. Figure 2(c) shows the F-N plots of four consecutive tests for a NanoLab carbon nanotube sample. The slope of first curve differs evidently from other three ones that are very closed. In following part, we will analyze in more detail about surface adsorption related emission performance for MWNT.

## **B. Emission stabilities of MWNT emitters**

### *a). Emission-adsorption equilibrium state and current stability*

Figure 4 shows the emission variation under several vacuum-atmosphere cycles for a MWNT sample. Emission currents were measured under 480 V with anode-emitter distance of  $\sim 300 \mu\text{m}$ . After exposing to air for 3 and 5 hours respectively, second current-time (I-t) test was started after pumping system 5 hours but third curve was acquired after 11 hours pumping. There are two noticeable phenomena from the tests. At first, currents normally drop after short pumping time and increase after longer pumping. Secondly, the drop or climb of the current started from the ends of the previous tests and mainly happened in the initial periods. We suggest adsorption molecule anticipated surface reactions play crucial roles on both effects. After short pumping, many of the nanotube surface adsorbents, mainly  $\text{H}_2\text{O}$ , could not be effectively released. There probably is a  $\text{H}_2\text{O}$  dominated adsorption layer at the start of the emitting test. Some  $\text{H}_2\text{O}$  molecule on emission sites may be released by the local temperature rise due to the electron emission Joule heating. *K. A. Dean et al*<sup>18, 19</sup> investigated the effects of water

adsorption on the field emission. They found that there is a water dominated adsorbate tunneling state that may increase the emission and the cleaning of the water will result in dramatic current drop. Thus the current decreased continuously in the initial period of second I-t test until the establishment of the surface emission-adsorption equilibrium state. Whereas after longer pumping, most of the surface contamination including H<sub>2</sub>O was desorbed. There is a big chance that the emission site surface is not totally covered by adsorbates. Normally in high vacuum condition, hydrogen is a main system residual gas component. It is probably that hydrogen molecule react with the emission surface during the emission. From our experiment, emission current from MWNT may increase in a 10<sup>-7</sup> Torr hydrogen surrounding. Thus, emission rose in this hydrogen anticipated reaction process until it reaches another emission-adsorption equilibrium state, as shown in 3<sup>rd</sup> I-t test of Fig. 4. After the formation of this equilibrium state, the surface-adsorbate bond should be stronger than ordinary physical adsorption bond. Even after sample experiences an atmosphere-vacuum cycles, this bond still stands and there is a small chance for other molecules to replace the adsorbate. This mechanism explains the continuity of two current tests separated by an atmosphere-vacuum cycle. Supply of external energy, like Joule heating from emission or heating sample directly, may destroy this bond.

*b). Influences of nitrogen or hydrogen on emission*

The influence of the nitrogen adsorption on field emission was investigated. In Fig. 5, nitrogen was introduced into the chamber to atmospheric pressure for about 5 hours after 1<sup>st</sup> emission stability test. 2<sup>nd</sup> test was conducted after pumping system for 1 hour

with pressure in low  $10^{-8}$  Torr. There is no evident current change between test 1 and test 2 except the natural emitting variation trend. This means that the interaction between MWNT surface and N is weak and nitrogen is easily desorbed after short pumping. This inertness makes nitrogen a good candidate as a protecting medium for the preservation of MWNT emitters.

Emission current increase was observed for metal emitters after operating in hydrogen atmosphere<sup>21, 22, 23</sup>, which appears to be due to the reduced work function of the emitter tip in the presence of hydrogen. In this work, the emission behavior of the MWNT emitters was investigated under operating samples in hydrogen atmosphere. Figure 6 shows the results for carbon nanotubes grown on Ni substrate by CVD method. Emission current increased after introducing the hydrogen into the system at 170<sup>th</sup> minute to raise the pressure up to  $1.3 \times 10^{-7}$  Torr. The current increased as high as ~10%, noted 7 hours after introducing hydrogen. This test shows the adsorption of hydrogen on the MWNT surface may improve the emission resulting from the reduction of work function, just like metal emitters. The fact the emission increased gradually after exposing to hydrogen could be related to a process in which surface molecules other than hydrogen are replaced by hydrogen molecules.

*c). Emission recovery effects by baking samples*

Based on the fact that water and other adsorbates play crucial role on the emission performance, the emission stability was investigated with baking system after exposing the sample to air. Figure 7 shows the results for MWNT sample that was grown on 304 stainless steel foils in our CVD system. After exposing sample to air for 3.5 hours and re-



testing the sample, the emission dropped 5 ~ 10%. Test 3 shows the emission recovery after baking the system to 150 °C for 12.5 hours. The sample experienced two periods of air exposures in test 4, in which emission current declined about 7% after introducing air to obtain  $5 \times 10^{-8}$  Torr pressure and dropped more than 30% after introducing air to  $4.7 \times 10^{-7}$  Torr for 13 hours. After baking the sample, emission recovered to ~ 95% of its previous value, as shown in test 5. Test 6 of operating sample under  $4.7 \times 10^{-7}$  Torr and test 7 of emission after baking the sample repeated the results of 4 and test 5. When MWNT sample emitted under  $3 \times 10^{-6}$  Torr air, current lost was as high as 70% in 14 hours as shown in test 7, but baking only recovered the emission to ~ 80% in test 8. Long-term operation of MWNT under high atmosphere pressure ( $4.7 \times 10^{-7}$  Torr and  $3 \times 10^{-6}$  Torr in our investigation) may cause permanent loss of emission. This may be caused by two reasons: a. damage of emitting sites by ion bombardment; b. surface physical and/or chemical states variation by gas adsorptions.

In order to identify the mechanism, we tested the emission stability for a similar MWNT sample with nitrogen exposure. After operations of MWNT emitters under  $3 \times 10^{-7}$  Torr and  $6 \times 10^{-6}$  Torr nitrogen atmosphere, the current loss, which is believed to be mainly caused by adsorptions of H<sub>2</sub>O and O<sub>2</sub> impurities, could be totally recovered after baking samples. This means that the ion bombardment under high pressure (up to  $10^{-6}$  Torr) operation doesn't cause significant emission degradation. To figure out the key adsorption component causing the current loss, system partial pressures after introducing air and nitrogen were analyzed by RGA. We found H<sub>2</sub>O partial pressures were  $7 \times 10^{-9}$  Torr and  $1.8 \times 10^{-8}$  Torr respectively after introducing  $4.7 \times 10^{-7}$  and  $3 \times 10^{-6}$  Torr air into system, and were  $3.5 \times 10^{-9}$  Torr and  $1.6 \times 10^{-8}$  Torr for purging  $3 \times 10^{-7}$  Torr and  $6 \times 10^{-6}$  Torr

nitrogen respectively. It is clear that H<sub>2</sub>O partial pressures are in the same degrees of magnitude for exposing nitrogen and air in our investigations. O<sub>2</sub> partial pressures, which were  $2.9 \times 10^{-8}$  Torr and  $2.1 \times 10^{-7}$  Torr for exposing  $6 \times 10^{-6}$  Torr nitrogen and air respectively, varied largely. We conclude that O<sub>2</sub> play a big role for the emission loss, which is probably caused by the emission site disappearances due to oxygen related chemical reaction during emission. It seems emission under O<sub>2</sub> partial pressures of higher than  $10^{-8}$  Torr is especially harmful. Generally, emission becomes more stable after baking the MWNT sample.

System pressure variation during a stability test is shown in Fig. 8 in  $10^{-10}$  Torr range for a MWNT sample that was treated by plasma etching. After a sharp increase at the moment of turning on the emitter, pressure, therefore the desorption rate of surface contaminations, gradually reached to the highest value in about two hours and then dropped to a stable level after three hours. The initial high degassing probably was mainly from the silicon collector surface. The following slow pressure rise could be a desorption process that is dominated by the release of nanotube surface adsorbates due to Joule heating.

## V. SUMMARY

Experimental results on the surface adsorption states related field emission performances are presented in this paper. F-N curves were used to interpret the surface adsorption states changes for W, Pt/Ir and MWNT emitters, and the change of the slopes shows clearly the process of desorption of the surface contaminations during emission.

Normally surface adsorption states tend to be stable after large amount of initial degassing, which is mainly produced by Joule heating.

Emission stability for the carbon nanotube samples is subject to change with various exposures and operating modes. Emission currents varied largely when MWNT emitters were exposed to atmospheric pressure. MWNT could emit repeatable currents after vacuum-atmosphere cycles if baking the sample in vacuum or allowing long enough gas desorption period. There may exist two different surface reaction modes in initial emission period, which are H<sub>2</sub>O and H<sub>2</sub> dominated processes respectively resulting from different surface water coverage. An emission-adsorption equilibrium state may form during the initial emission period, and the stronger surface-adsorbate bonds in this state probably result in the current continuity between two tests separated by an atmosphere-vacuum cycle. Supply of external energy, like Joule heating from emission or heating sample directly, may destroy this bond. Nitrogen gas is a good protecting environment to maintain emission stability during the vacuum-atmosphere cycle. Operations of MWNT emitters under hydrogen atmosphere improve the emission, which could be related to the modification of the surface work function. We suggest that surface adsorbate participated reaction, where oxygen is believed to play a key role, is the dominated factor for the emission losses under pressure operation.

### **Acknowledgement**

This work was carried out under a Cooperative Research and Development Agreement between the U.S Department of Energy's Thomas Jefferson National Accelerator Facility (DOE contract DE-AC05-84ER40150), Varian Vacuum Technologies and Old Dominion

University. The authors would like to thank Mr. B. Roberdtson for technical assistances, Mrs. H. Wang for plasma etching and Mrs. T. Wang for SEM measurements.

### List of references

- <sup>1</sup> W.P. Dyke and J. K. Trolan, *Phys. Rev.* **89**, 799 (1953)
- <sup>2</sup> E.E. Martin, J.K Trolan, and W.P. Dyke, *J. Appl. Phys.* **31**, 782 (1960)
- <sup>3</sup> A.V. Crewe, D.N. Eggenberger, J. Wall, and L.M. Welter, *Rev. Sci. Instr.* **39**, 576 (1968)
- <sup>4</sup> L.W. Swanson and L. C. Crouser, *J. Appl. Phys.* **40**, 4741 (1969)
- <sup>5</sup> Walt A. de Heer, A. Chatelain, D. Ugarte, *Science* **270**, 1179 (1995)
- <sup>6</sup> Shoushan Fan, Michael G. Chapline, Nathan R. Franklin, Thomas W. Tombler, Alan M. Cassell, Hongjie Dai, *Science* **283**, 512 (1998)
- <sup>7</sup> W. Zhu, C. Bower, O. Zhou, G. Kochanski, and S. Jin, *Appl. Phys. Lett.* **75**, 873 (1999)
- <sup>8</sup> Hirohiko Murakami, Masaaki Hirakawa, Chiaki Tanaka, and Hiroyuki Yamakawa, *Appl. Phys. Lett.* **76**, 1776 (2000)
- <sup>9</sup> Robert Gomer, *Field emission and field ionization*, American Institute of Physics, New York, 1993
- <sup>10</sup> R.H. Fowler and L.W. Nordheim, *Proc.R.Soc.London, Ser.A* **119**, 173 (1928)
- <sup>11</sup> C. A. Spindt, I. Brodie, L. Humphrey, and E. R. Westerberg, *J. Appl. Phys.* **47**, 5248 (1976)
- <sup>12</sup> O.Groning, O.M.Kuttel, Ch. Emmenegger, P. Groning, and L. Schlapbach, *J.Vac.Sci.Technol. B* **18**, 665 (2000)

- <sup>13</sup> W.P. Dyke, F.M. Charbonnier, R.W. Strayer, R.L. Floyd, J.P. Barbour, and J. K. Trolan, *J. Appl. Phys.* **31**, 790 (1960)
- <sup>14</sup> I. Brodie and C.A. Spindt, *Vacuum Microelectronics*
- <sup>15</sup> J.A. Becker, *Advances in Catalysis* **7**, 136 (1955)
- <sup>16</sup> A. Cricenti, E. Paparazzo, M.A. Scarselli, L. Moretto, and S. Selci, *Rev. Sci. Instrum.* **65**, 1558 (1994)
- <sup>17</sup> P.R. Schwoebel and C.A. Spindt, *Appl. Phys. Lett.* **63**, 33 (1993)
- <sup>18</sup> Kenneth. A. Dean and Babu R. Chalamala, *Appl. Phys. Lett.* **75**, 3017 (1999)
- <sup>19</sup> Kenneth. Paul von Allmen, and A. Dean and Babu R. Chalamala, *J. Vac. Sci. Technol. B* **17**, 1959 (1999)
- <sup>20</sup> Hugh O. Pierson, *Handbook of Carbon, Graphite, Diamond and Fullerenes*, Noyes Publications, Park Ridge, New Jersey, 1993, p64
- <sup>21</sup> P. R. Schwoebel and C.A. Spindt, *Appl. Phys. Lett.* **63**, 33 (1993)
- <sup>22</sup> S. Itoh, T. Niiyama, and M. Yokoyama, *J. Vac. Sci. Technol. B* **11**, 647 (1993)
- <sup>23</sup> Changkun Dong and G. Rao Myneni, *J. Vac. Sci. Technol. A* **17**, 2026 (1999)

## List of figure captions

Fig. 1 SEM pictures of carbon nanotube samples. a) MWNT grown on Hastelloy; b) Commercial NanoLab MWNT sample.

Fig. 2 Slope variations of F-N curves for metal and carbon nanotube emitters. a) Tungsten single tip; b) Pt / Ir single tip; c) MWNT sample.

Fig. 3 System pressure variation with different test cycles under emission current of 2  $\mu\text{A}$  for Pt/Ir single tip.

Fig. 4 Emission variation with different pumping periods after exposing to air. 1<sup>st</sup> test was conducted after overnight baking sample; 2<sup>nd</sup> test (3<sup>rd</sup> test) was measured after exposing sample to air for 3 hours (5 hours) then pumping system for 5 hours (11 hours).

Fig. 5 Emission with exposing MWNT sample to nitrogen. 1<sup>st</sup> test was conducted after overnight baking sample; 2<sup>nd</sup> test was measured after exposing sample to atmospheric pressure nitrogen for 5 hours then pumping system for 1 hour.

Fig. 6 Emission stability with / without exposing MWNT sample in hydrogen. In the period of 0 to 170 minute, system was under  $2 \times 10^{-9}$  Torr vacuum without introducing hydrogen; afterwards, hydrogen was introduced to raise pressure to  $1.3 \times 10^{-7}$  Torr.

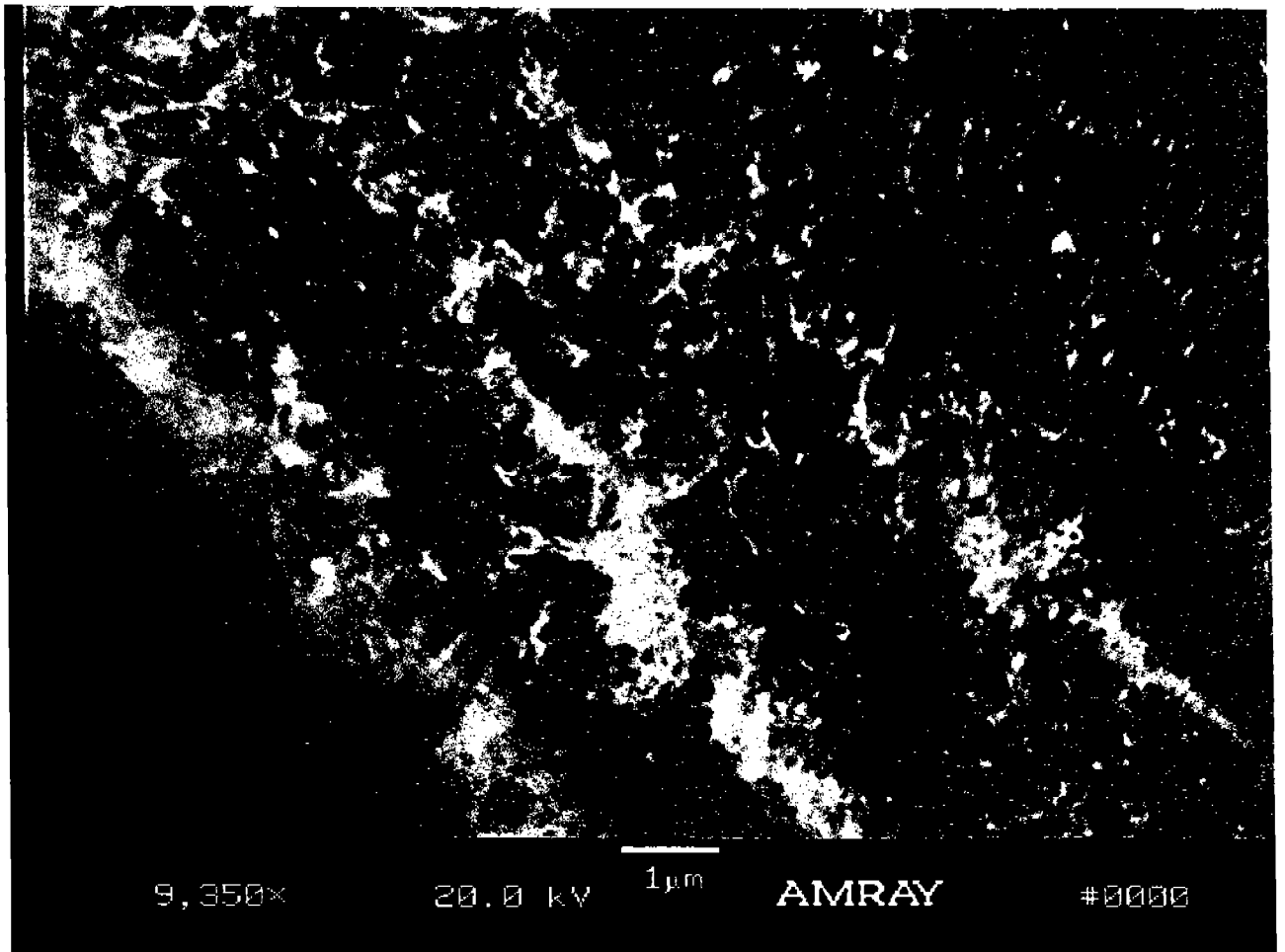


Fig. 1 (a) — Doney, Gupta, Mysore

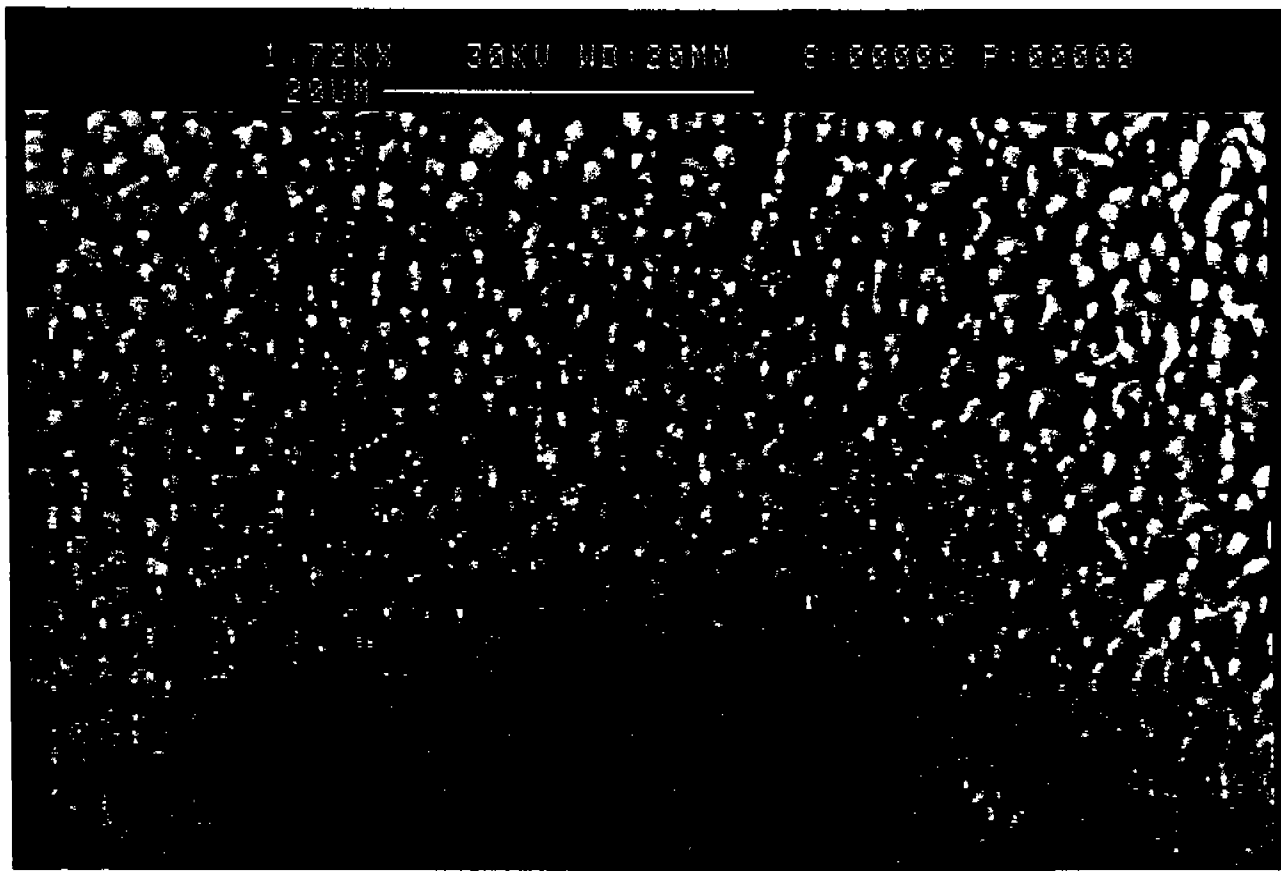


Fig-1 (b) - Dong, Gupta, Myneni



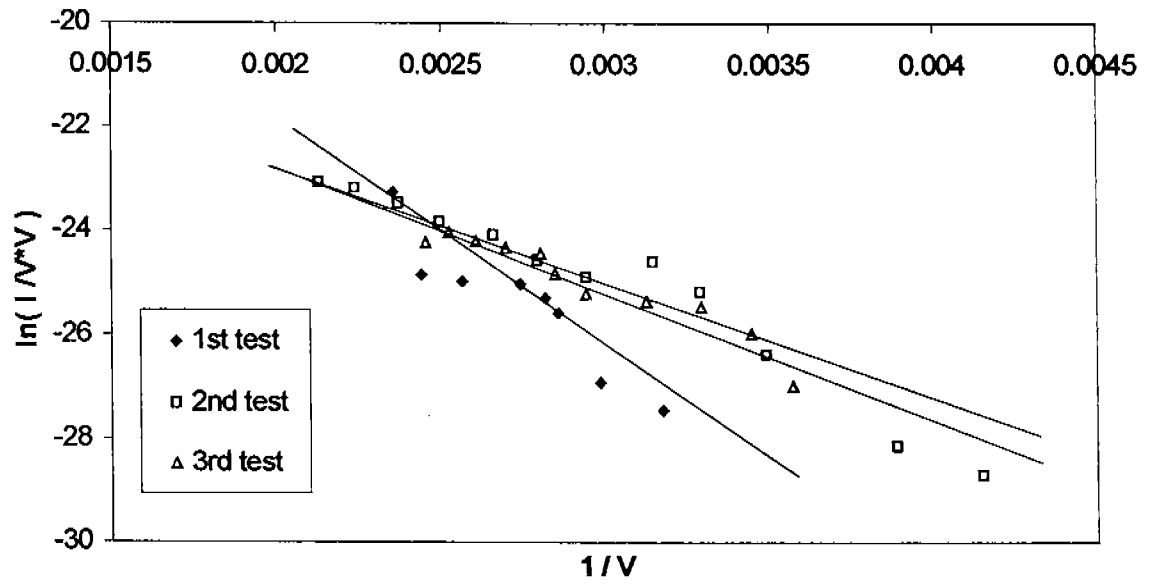


Fig-2 (a) - Dong, Gupta, Myneni

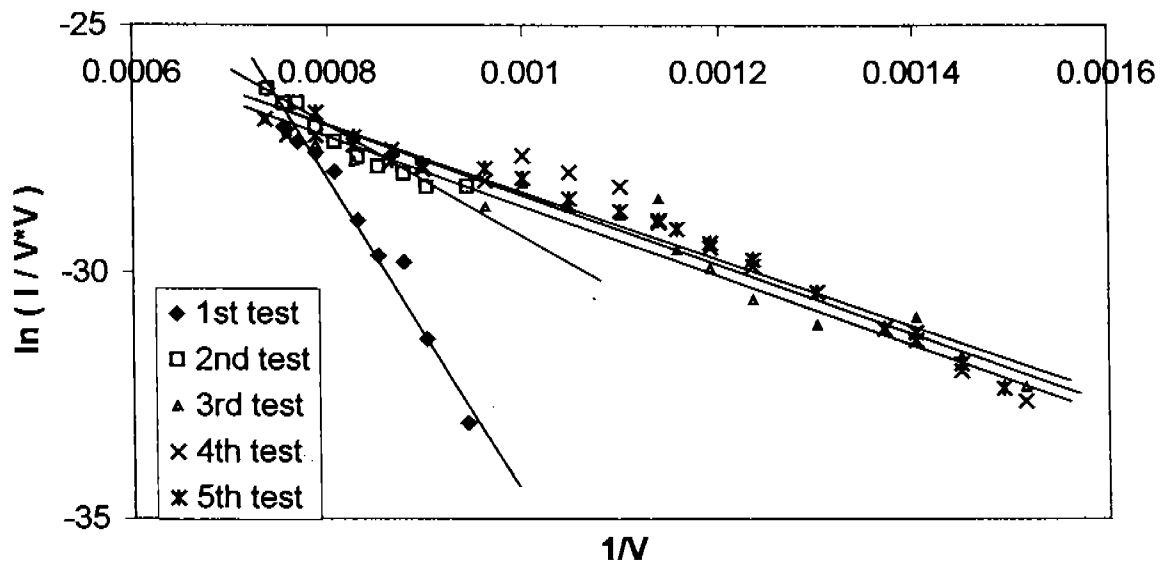


Fig. 2 (b) - Dong, Gupta, Alyaeni

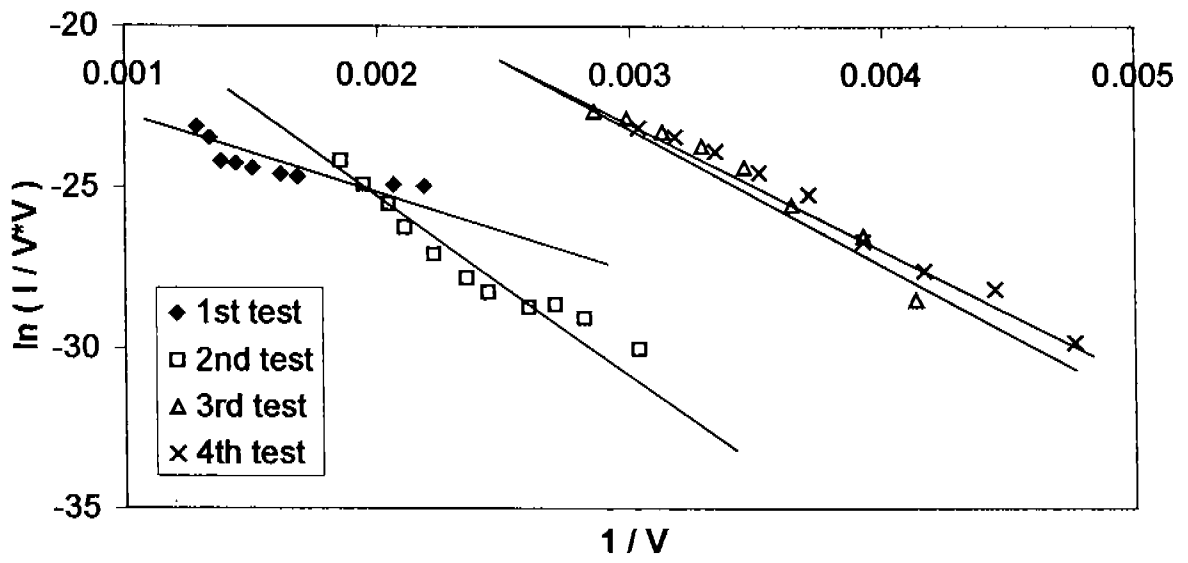


Fig-2 (c) - Dong, Gupta, Myneni

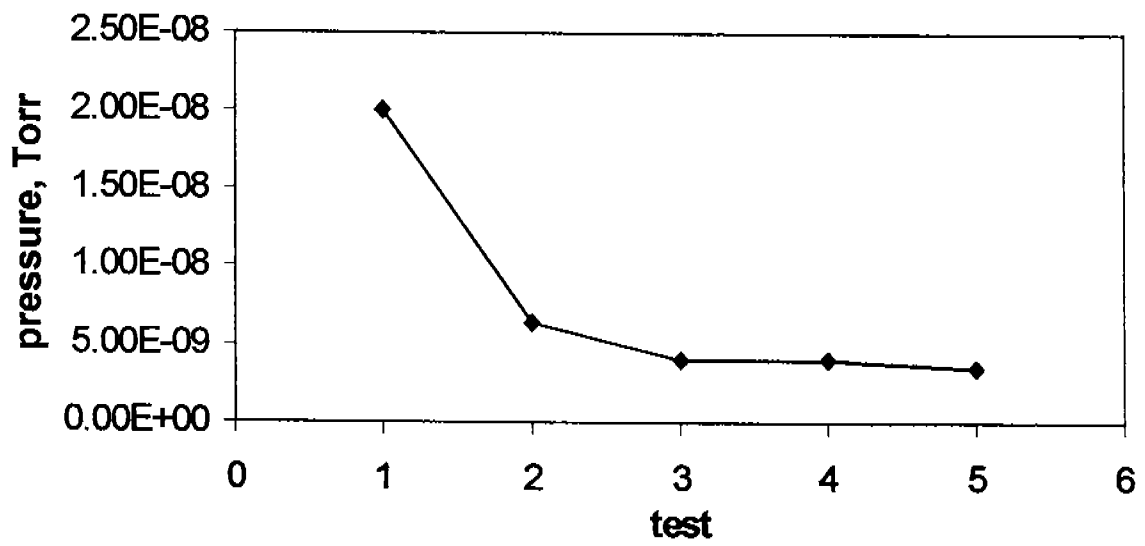


Fig-3 - Deng, Gupta, Myneni

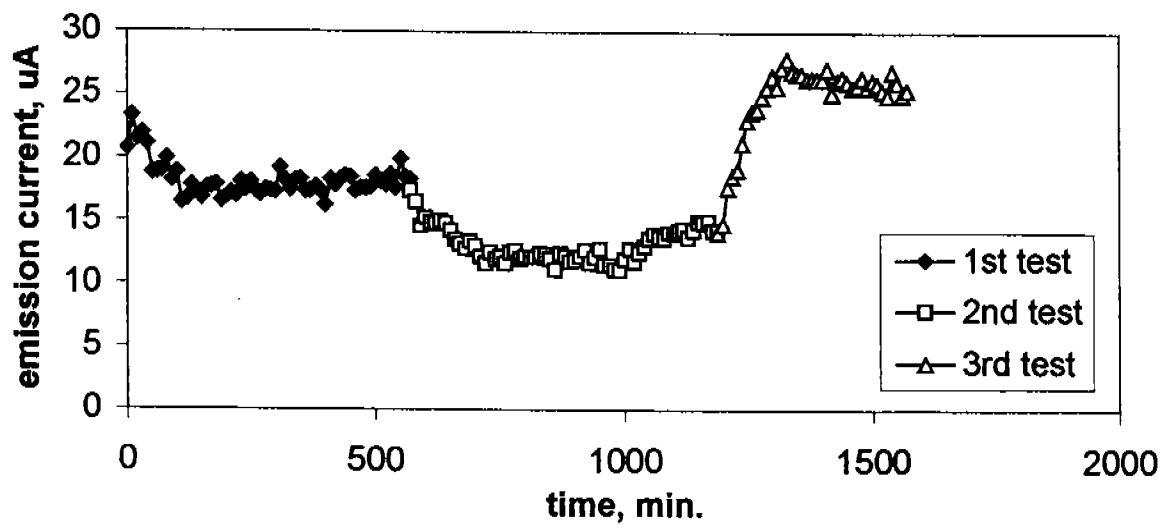


Fig.4 - Dong, Gupta, Myneni

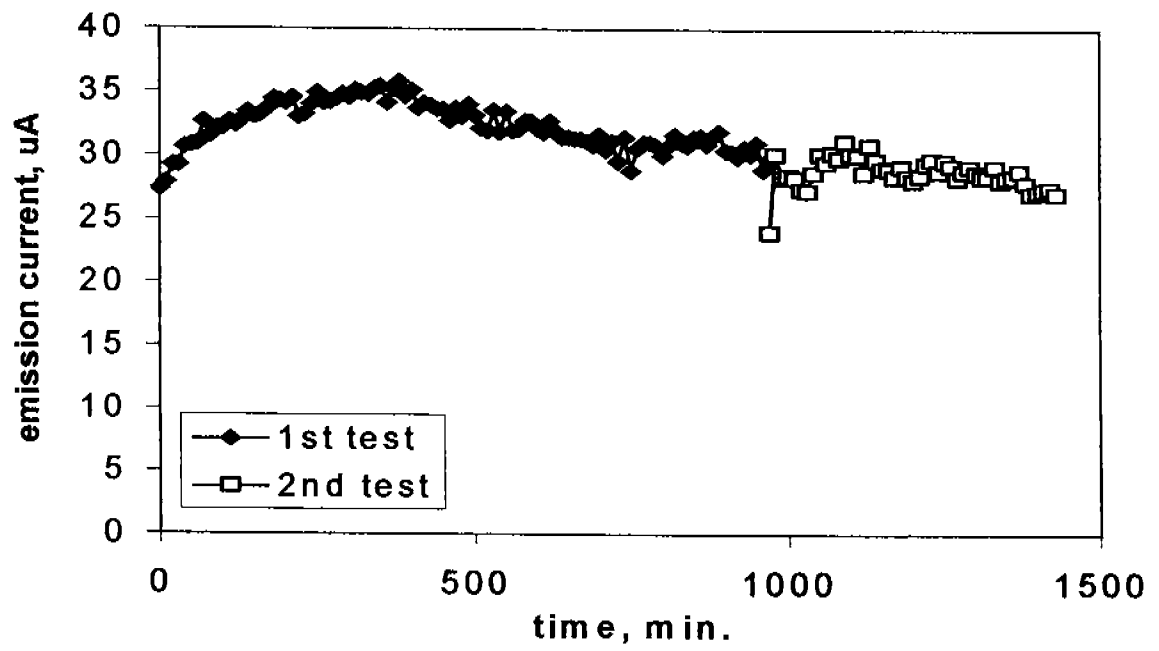


Fig-5 - Dong, Gupta, Myneni

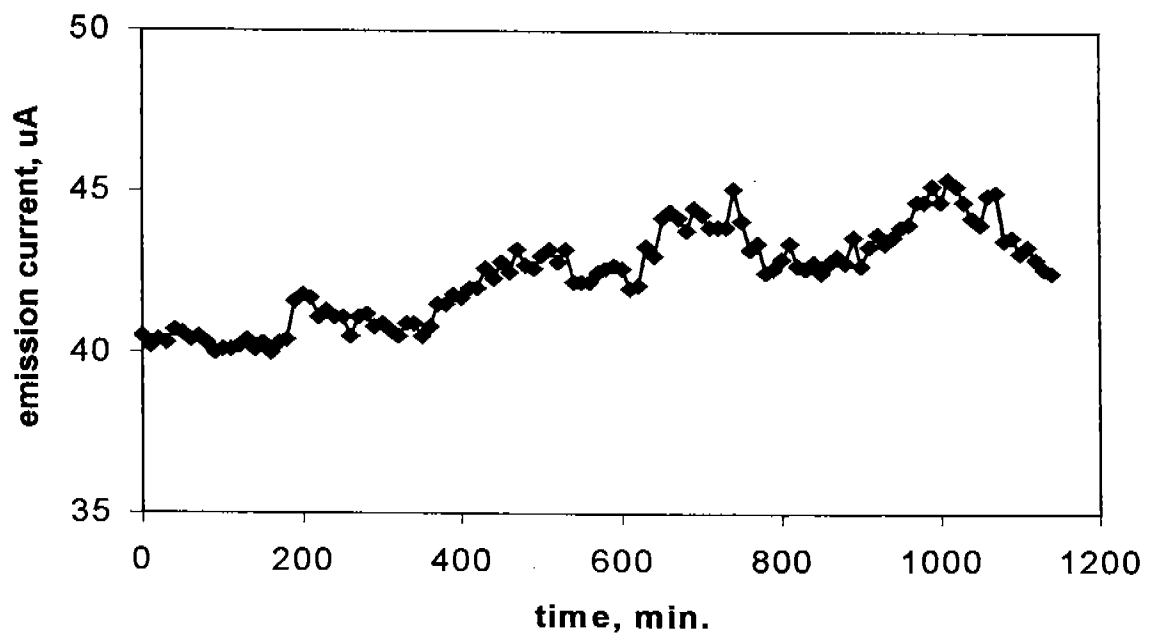


Fig. 6 - Dong, Gupta, Myneri

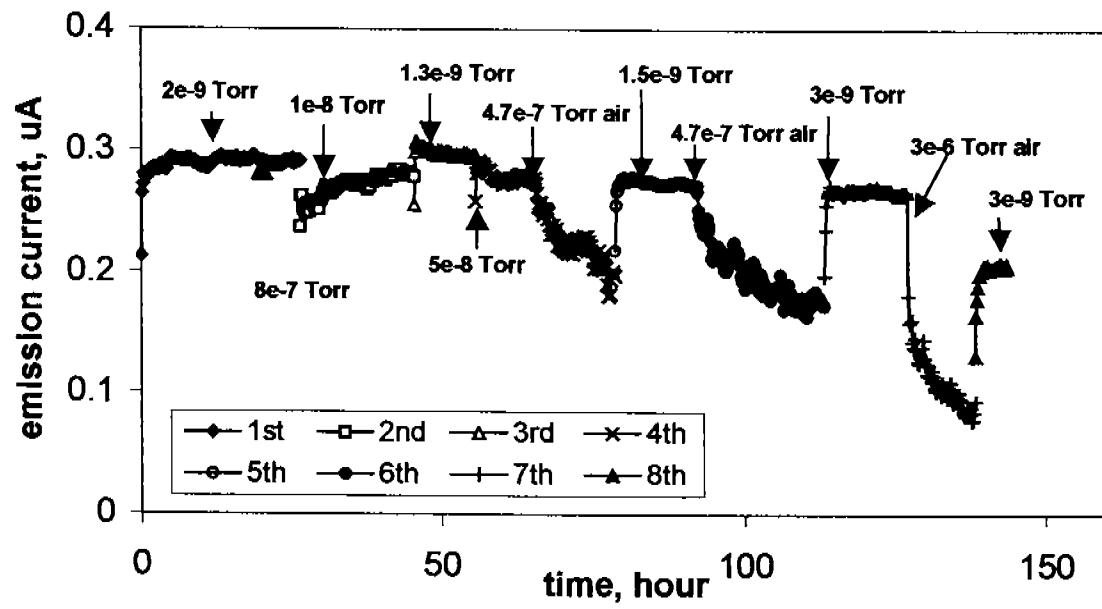


Fig. 7 - Dong, Gupta, Myneni



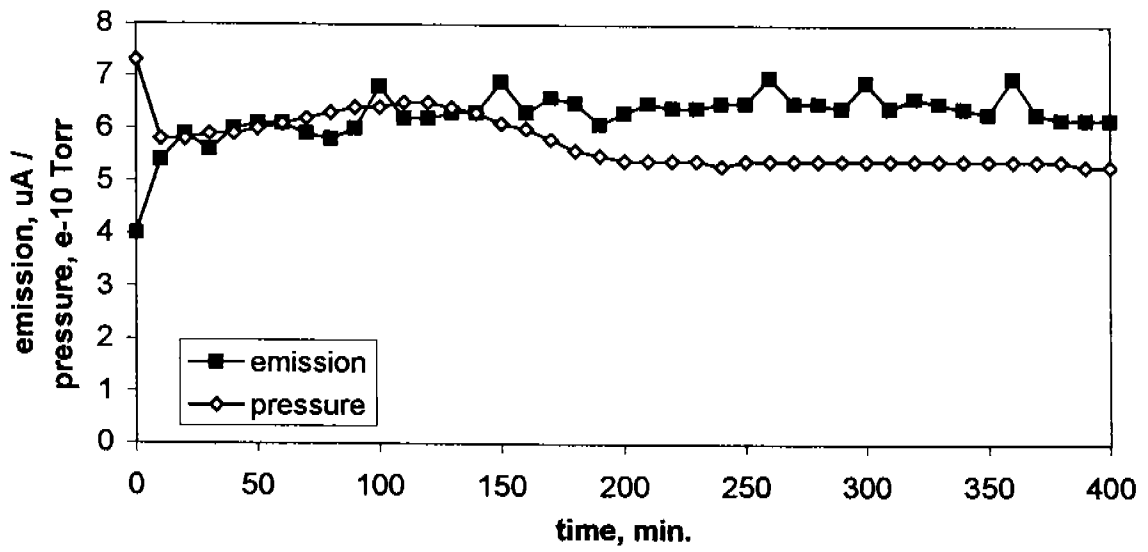


Fig. 8 - Dong, Gupta, Myneni